

Dynamic System-Level Simulation of Dynamic Frequency Planning for Real Time Services in WiMAX Networks

David López-Pérez
Centre for Wireless Network
Design
Bedfordshire University
Luton, UK
David.Lopez@beds.ac.uk

Alpár Jüttner
Centre for Wireless Network
Design
Bedfordshire University
Luton, UK
Alpar.Juttner@beds.ac.uk

Jie Zhang
Centre for Wireless Network
Design
Bedfordshire University
Luton, UK
Jie.Zhang@beds.ac.uk

ABSTRACT

This paper introduces a dynamic system-level simulator for WIMAX (*Wireless Interoperability for Microwave Access*) networks that can be used to analyze the behavior of several network procedures. Moreover, the performance of a new approach to the frequency assignment problem, called DFP (*Dynamic Frequency Planning*), is studied using this simulation platform. DFP is able to run from a few times a day down to a frame by frame basis, balancing the radio resources between neighbouring BSs (*Base Stations*) and providing interference mitigation. We demonstrate the efficacy of DFP compared to off-the-shelf FRSs (*Frequency Reuse Schemes*) in terms of average network capacity and delay.

Categories and Subject Descriptors

C.4 [Performance of Systems]: Metrics—*Design studies, modeling techniques, reliability and availability*

General Terms

Algorithms, Design, Performance.

Keywords

Dynamic frequency planning, WiMAX, OFDMA

1. INTRODUCTION

WiMAX is appointed by the industry as one of the most suitable wireless communication systems for satisfying the growing user demands. It relies on an all-IP architecture, and provides high *QoS* (*Quality of Service*) and data rates. WiMAX (IEEE 80211.16-2005) [1] is based on a scalable OFDMA (*Orthogonal Frequency Division Multiple Access*) PHY (*PHYsical*) layer, which provides different benefits to the network such as robustness against multi-path, high spectral efficiency, simple implementation, etc.

Permission to make digital or hard copies of all or part of this work for personal or classroom use is granted without fee provided that copies are not made or distributed for profit or commercial advantage and that copies bear this notice and the full citation on the first page. To copy otherwise, or republish, to post on servers or to redistribute to lists, requires prior specific permission and/or a fee. *IWCMC'09*, June 21-24, 2009, Leipzig, Germany. Copyright ©2009 ACM 978-1-60558-569-7/09/06 ...\$5.00

In order to avoid inter-cell interference, OFDMA networks are flexible in terms of radio frequency planning and they support a large variety of FRSs. These techniques will reduce inter-cell interference by assigning different fragments of the available channel to different sectors of the network [2]. However, these fix FRSs are not the most suitable solution to achieve an optimal network performance in dynamic scenarios, where the network load and user traffic continuously change. This fact is an especially true in scenarios where the traffic load is high and inhomogeneously distributed.

In [2], the authors study the performance of an OFDMA system under the classic and fix frequency reuse patterns (reuse 1, reuse 3, and fractional reuse 1-3) by computer simulations. This analysis is performed over an ideal and regular grid of BSs, which is far away from realistic network deployments. In [3], similarly to the previous work, the authors compare the performance of an OFDMA system under the classic FRSs. They also propose a new scheme, called partial isolation, which is a mix of these classical approaches and power control algorithms. However, this technique is still based on fix frequency patterns that are not able to adapt the bandwidth of the sectors to the traffic requirements.

In this paper, the performance of a new resource balancing technique called DFP is compared to the traditional FRSs: reuse factor 1 and 3. This approach was presented in [4], and therefore the target of this work is not to introduce this technique, but check its performance using a new dynamic system-level simulator.

DFP dynamically adapts the radio frequency resources of the OFDMA PHY layer of each BS to the changing conditions of the wireless channel and the varying traffic of the customers. In order to analyze the performance of DFP under truly dynamic conditions, dynamic system-level simulations for WiMAX networks using real time services: *VoIP* (*Voice over IP*) and H.263 video are carried out. This kind of real time services are challenging DFP because the resources demanded by the users change on a frame basis.

The rest of the paper is organized as follows: Section II introduces the DFP algorithm. Section III describes the dynamic WiMAX system-level simulation. Section IV summarizes the traffic models used for VoIP and Video. Section V presents a performance comparison between DFP and 2 FRSs. Finally, in Section VI, the conclusions are drawn.

⁰This work is supported by the EU FP6 "RANPLAN-HEC" project on 3G/4G radio access network design under the grant number MEST-CT-2005-020958 and by COST293.

2. DYNAMIC FREQUENCY PLANNING

DFP [4] is a novel approach to the frequency assignment problem tailored to OFDMA networks, e.g., Mobile WiMAX. This approach is designed to cope with inter-cell interference in scenarios where the load of the network is inhomogeneously distributed and the traffic of the users changes rapidly. This technique allows an on-line allocation of the bandwidth to the BSs, e.g., a congested sector can borrow sub-channels from the neighbouring sectors if they have idle resources available. In addition, it also permits an efficient reuse of the OFDMA sub-channels throughout the network.

To model the DFP problem, let us first define an OFDMA network as a set of N sectors $\{S_0, S_i, S_j \dots S_{N-1}\}$, and K sub-channels $\{1, k \dots K-1\}$, where at each time T_{DFP} each sector S_i requires a certain number of sub-channels D_i .

Then, the DFP problem consists on assigning a certain number of sub-channels D_i to each sector S_i every T_{DFP} , while minimizing the global system interference. The interference restrictions between different sectors must be taken into account. Since the number of required sub-channels is usually larger than what is available, sub-channel reuse is needed.

Prior to solving the DFP problem, the inputs must be calculated [4], i.e. the demands vector and restriction matrix.

- *Demands Vector*

The demands vector $D[N]$ estimates the number of needed sub-channels D_i per sector S_i required to satisfy the radio resources demand of the users. This information can be a priori calculated, since each sector knows: 1) the number of connected users, 2) their requirements in terms of bandwidth and throughput, 3) and their interference conditions due to the channel quality indicator reported in previous frames.

- *Restriction Matrix*

The restriction matrix $W[N, N]$ approximates the inter-cell interference between the sectors of the network $w[i, j]$ in terms of the percentage of interference time. The model used for sensing the environment and estimating the inter-cell interference is based on *MRs (Measurement Reports)* and the *Coupling Matrix* [5].

In this approach, the terminals periodically send MRs to the serving BSs. The MR indicates the received signal strength *RxLev* of the serving cell S_i , as well as the stronger neighboring ones S_j . These signal levels are estimated according to the BS preambles.

Every time a MR is received by S_i , it increases the MR counter ($MR_i ++$). Moreover, if the offset between the signal level of S_i and S_j satisfies condition (1), S_i also increases the interference event counter ($Interf_{i,j} ++$).

$$RxLev_i < RxLev_j + Thres \quad (1)$$

where $Thres$ is an interference margin defined by the operator ($Thres = 12 \text{ dB}$).

After certain time, the percentage of interference time between S_i and S_j is can be computed as:

$$w[i, j] = \frac{Interf_{i,j}}{MR_i} \quad (2)$$

Once the inputs of the DFP are obtained, the frequency assignment problem can be model as a Mixed Integer Pro-

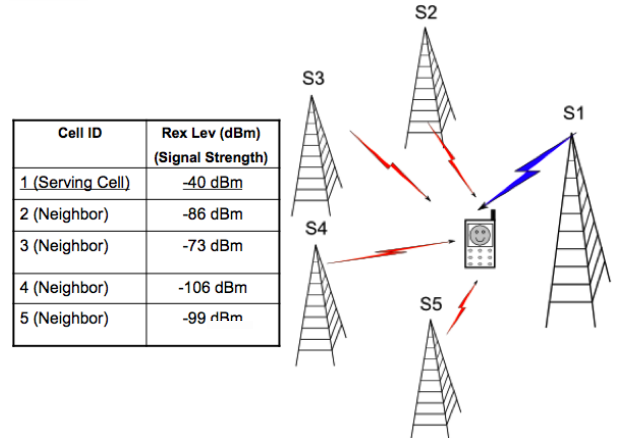


Figure 1: Measurement report.

gramming problem as follows (3), where the target is to find the optimal solution that minimizes the given cost function. This cost function represents the overall network interference.

$$\min \sum_{i=0}^{N-1} \sum_{j=0}^{N-1} \sum_{k=0}^{K-1} \frac{w_{i,j}}{D_i \cdot D_j} \cdot y_{i,j,k} \quad (3a)$$

subject to:

$$\sum_{k=0}^{K-1} x_{i,k} = D_i \quad \forall i, k \quad (3b)$$

$$x_{i,k} + x_{j,k} - 1 \leq y_{i,j,k} \quad \forall i, j, k \quad (3c)$$

$$y_{i,j,k} \geq 0 \quad \forall i, j, k \quad (3d)$$

$$x_{i,k} \in \{0, 1\} \quad \forall i, k \quad (3e)$$

where $x_{i,k}$ indicates that sector S_i uses the k th frequency. Constraint (3b) imposes that sector S_i uses D_i sub-channels. Inequalities (3c) and (3d) together force that in an optimal solution: $y_{i,j,k} = 1$ if and only if both sectors S_i and S_j use frequency k , and $y_{i,j,k} = 0$ otherwise.

Finally, the cost function is the sum of the interference between all pair of sectors S_i, S_j and all the frequencies k . To estimate the percentage of time that both sectors S_i, S_j are transmitting using the same frequency k at the same time, the interference restrictions $w_{i,j}$ must be divided by the number of used sub-channels D_i, D_j for both sectors S_i, S_j .

Many different approaches can be proposed to find the optimal or at least a good solution for the DFP problem in a macrocell environment. Three different approaches based on simulated annealing, tabu search and greedy algorithms has been proposed in [4]. Heuristics will find slightly higher quality solutions than greedy algorithms when solving DFP, but at the expense of longer running times. Therefore, when using DFP in an on-line scenario, it may be worth using faster algorithms since they produce only slightly worse solutions.

In this case, to cope with the dynamic behaviour of real time services, we will use the seven greedy algorithms proposed in [4] to solve the DFP problem. They run so fast that we can afford to run the seven algorithms and choose the best solution.

3. DYNAMIC SYSTEM-LEVEL SIMULATION

The dynamic system-level simulator presented in this section is focus on the analysis of OFDMA/TDD (*Time Division Duplex*) WiMAX networks, more in detail, on the performance of its *MAC (Medium Access Control)* and *PHY* layers. Each iteration represents one OFDMA frame and it includes features such as traffic generation, user connection, scheduling, *RRM (Radio Resource Management)*, burst transmission/reception, and channel state feedback among others. Note that mobility models are not used in this simulation, since handover analyses are out of the scope of this paper. For the sake of simplicity, only the *DL (DownLink)* module is presented. In the following, the simulation flow is described.

3.1 Initialization

In this module, the network configuration and the simulation parameters are fed in, e.g. antenna and propagation models, building and terrain data, BS and *UE (User Equipment)* information, service types, user profiles and traffic maps.

3.2 Path loss and fading calculation

In this platform, in order to model the radio channel between the BS and the UE, the path-loss, shadow fading and multi-path fading are considered.

Hata, FDTD [6] and Ray Tracing [7] models can be used here to compute the path-loss, each one with different features. Hata models are more suitable for broad analysis where the accuracy of the prediction is not an issue. Contrary, FDTD and Ray Tracing models produce more accurate results at the expense of the running time. All these models are tuned for working at $f = 3.5 \text{ GHz}$.

In addition, a log-normal distribution is used to model the shadowing effects, while *SUI (Stanford University Interim)* models are used to model the fast variations of the signals due to multi-path and the frequency selective fading. Note that a single shadow fading value and a set of K multi-path fading values are generated for each UE and OFDMA frame.

3.3 User Generation

In this module, the traffic load of the network is updated according to a Poisson process [8]. The probability of the arrival of n new sessions is given by:

$$p_n(T) = \frac{(\lambda T)^n}{n!} e^{-\lambda T} \quad (4)$$

where $T[s]$ and $\lambda[ue/km^2 \cdot s]$ denote the sampling period and the average arrival rate per area, respectively.

For each new session, the holding time t_H is described by an exponential distributed random variable generated from the next PDF:

$$f_{t_H}(t_H) = \mu e^{-\mu t_H} \quad (5)$$

where μ denotes the mean holding time.

To simulate different service densities within a traffic map, different values of λ and μ can be defined per service type.

3.4 Best Server and Preamble Decoding

Once that a new session is generated, the UE and the network attempt to connect with each other through a BS. The UE selects the sector, which provides the best received

pilot signal strength as a server, where this parameter must be larger than the sensitivity of the antenna of the UE.

After the best server of the user is identified, a connection is set up between them. This connection is defined by the pair: *CID (Connection Identifier) / SFID (Service Flow Identifier)* where the CID denotes the unique identity of the connection and the SFID refers to the QoS features of it.

After the connection is established, the UE estimates the signal quality of all the sub-channels of the BS preamble. Then, the UE feeds back this information to the BS, which will use it to select the appropriate user profile for the transmission.

Table 1: WiMAX User Profiles [9]

RAB	Modulation	Code rate	SINR [dB] threshold	Efficiency bit/symbol
RAB1	QPSK	1/2	2.88	1.00
RAB2	QPSK	3/4	5.74	1.50
RAB3	16QAM	1/2	8.79	2.00
RAB4	16QAM	3/4	12.22	3.00
RAB5	64QAM	1/2	15.88	4.00
RAB6	64QAM	3/4	17.50	4.50

3.5 Traffic Generation

The traffic generator agent is considered as an upper layer application that generates *MAC-SDUs (Service Data Unit)*. These MAC-SDUs are created according to different traffic models that vary depending on the service type (Section 4). These MAC-SDUs are inserted into a queue, which is associated to the UE connection, after the mapping CID/SFID.

Note that when using real time services, the MAC-SDUs that are not transmitted at the required time will be deleted from the CID/SFID queue, and the packets will be discarded.

3.6 ARQ Block Generation

The MAC-SDU are fragmented into MAC-ARQ blocks if the *HARQ (Hybrid Automatic Repeat Request)* mechanism is enabled in the given CID/SFID connection [10]. The size of the MAC-ARQ can be selected from the following set: {64, 128, 256, 512, 1024, 2048}[bytes] [11].

3.7 Scheduling and Quality of Service

First of all, the MAC scheduler classifies the different connections into different traffic classes. Each traffic class has its own priority, sorted here in decreasing order: *UGS (Unsolicited Grant Services)*, *rtPS (real-time Polling Services)*, *ErtPS (Extended real-time Polling Services)*, *nrtPS (non-real-time Polling Services)* and *BE (Best Effort)*.

Afterwards, the MAC scheduler classifies the connections within the same traffic class applying a scheduling policy. This simulation platform supports three different strategies: *FIFO (First In First Out)*, *Best SINR (Signal to Interference plus Noise Ratio)* and *PF (Proportional Fair)*. When using FIFO, the connections that were created first have the highest priority. On the other hand, best SINR and PF make use of the channel quality information fed back in previous frames to classify the connections. The best SINR policy tends to increase the network throughput, since the

UEs which larger SINRs (close to the BS) are scheduled first. The PF policy tends to increase the fairness between the users, since the UEs with larger ratio current to average SINR are scheduled first. The SINR history of a UE is recorded in a moving window.

3.8 Radio Resource Management

First of all, the ARQ blocks of the user, which is appointed by the scheduler, are fragmented or concatenated into MAC-PDUs (*Packet Data Unit*). The size of the MAC-PDU can be selected from the next set: {64, 128, 256, 512, 1024, 2048} [bytes].

Afterwards, resources are allocated to the UE by the BS for satisfying its bandwidth demand, while achieving its QoS requirements taking the channel conditions into account [12].

The minimum resource that can be allocated by the BS is the *slot*, which consists of one sub-channel and one, two or three OFDM symbols, depending on the network configuration. Note that the sub-channels maybe built by using either contiguous or pseudo-random distributed sub-carriers.

Slots built of contiguous sub-carriers, *AMC (Adaptive Modulation and Coding)*, are suitable for those users, whose channel conditions change slowly across the sub-channels over time, since the BS can exploit multi-user diversity.

Slots built of distributed sub-carriers, *PUSC (Partial Usage of Sub-Channels)*, are suitable for those users, whose channel conditions vary quickly over the frequency and time, since the BS can take advantage of frequency diversity.

The resources are allocated to the UE by the BS in a form of *burst*, which is a two dimensional (frequency/time) data region of contiguous slots. Since the number and size of the ARQ blocks to be transmitted are known by the BS, and also the modulation and coding scheme to be assigned to each UE (Table 1), the BS can compute how many slots are need to served each user, and then, build its burst.

The BS will allocate as many slots as needed to accommodate the minimum number of PDUs that satisfies the minimum required throughput of the user service (fair approach). If after serving all users there are still resources left, the burst of the user is expanded with more PDUs. What slots are allocated to the UE depend on the resource allocation strategy. In this work, 3 different resource allocation strategies for interference mitigation are used: reuse 1, reuse 3 and DFP.

These FRSs are given for comparison and described by the notation $N_c \times N_s \times N_f$, where N_c denotes the number of channels, N_s indicates the number of sectors per BS, and N_f shows the fragments number in which the channel is divided.

When using $1 \times 3 \times 1$ (Figure 2), there is only one radio channel available and each BS of the network has 3 sectors. Afterwards, every sector of the network is allowed to use all the sub-channels within the radio channel. Using this FRS, no frequency planning is needed, simplifying the task of the operator, but the chance of inter-cell interference coordination is then neglected.

When using $1 \times 3 \times 3$ (Figure 2), the channel is divided in three segments and each segment is assigned to each sector. This scheme simplifies the radio frequency planning design, since the operator only needs to assign segments to sectors. Additionally, this FRS mitigates inter-cell interference by reducing the probability of slots collision by a factor of 3. However, the sector capacity is reduced by a factor of 3 too.

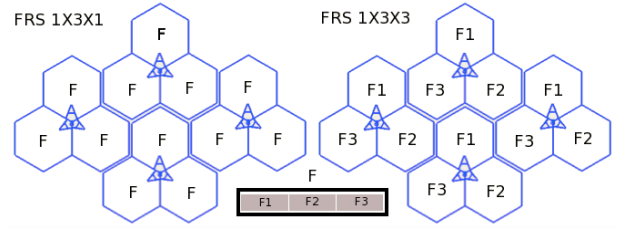


Figure 2: Frequency Reuse Scheme.

3.9 Power Resource Management

Since the focus of this work is the analysis of sub-channel allocation techniques, a simple but realistic power allocation strategy has been considered. The power P_i of a macrocell S_i is equally distributed among all its existing pilot and data sub-carriers ($R_{pilot} + R_{data}$), in the following way:

- If sub-channel k is busy, a power $P_i / (R_{pilot} + R_{data})$ is applied to each one of its data sub-carriers.
- If sub-channel k is idle, no power is applied.

3.10 Transmission and SINR calculation

Once the RRM module has built the ODFMA frames, they are transmitted from the BSs to the UEs. Interference will happen when the signals of several UEs overlap in the frequency (sub-channel) and time (slot) domain. For the sake of simplicity, a perfect synchronization is assumed between all the BSs. Therefore, inter-cell interference will occur when several UEs use the same sub-channel/symbol. Note that intra-cell interference has been neglected due to the orthogonality features of the OFDMA sub-carriers.

To compute the SINR value of each slot (x th sub-channel y th symbol) of each BS, the next model is used:

$$SINR_{x,y,i} = \frac{P_{x,y,i} \cdot PL_{i,m} \cdot GL_{i,m}}{\sum_{j=0, j \neq i}^N (P_{x,y,j} \cdot PL_{j,m} \cdot GL_{j,m}) + \sigma} \quad (6)$$

where $m = UE_{x,y,i}$ and $P_{x,y,i}$ denote the user and power allocated in the x th sub-channel and y th symbol of the i th BS. $PL_{k,UE_{x,y,i}}$ indicates the path-loss, shadowing and multipath fading attenuation. $GL_{k,UE_{x,y,i}}$ indicates the gains and losses between k and m , e.g., antenna gain, cable loss, noise figure. Finally, σ makes reference to the background noise experienced by the sub-channel.

3.11 ARQ block decoding

The SINR of each ARQ block is calculated as the average SINR value of the slots in which the ARQ block is fitted in. *MIC (Mean Instantaneous Capacity)* is used to compute this average $SINR_{ARQ}$ value [13].

Then, if the ARQ block is a re-transmitted version of a previous ARQ block, the SINR of the ARQ block is recalculated. This is due to the HARQ mechanism. In this case, a *CC (Chase Combining)* model is used to perform this task [14]:

$$SINR_{eff} = \epsilon^R \cdot \sum_{r=0}^R SINR_{ARQ}(t-r) \quad (7)$$

where R denotes the number of retransmissions and ϵ represents the losses due to the combination of the ARQ blocks. Note $\epsilon = [0.2 - 0.3]dB$.

Once the $SINR_{eff}$ of each ARQ block is calculated, the BS decides if this block was transmitted with an error or not. To take this decision, the BS compares the $SINR_{eff}$ of the ARQ block with an SINR threshold. When the $SINR_{eff}$ of the ARQ block is larger than the threshold, the BS assumes that the packet is transmitted successfully; otherwise the BS assumes that the packet is erroneous, and it asks for a retransmission.

Note that link-level simulations [12] and a random variable uniformly distributed between 0 and 1 [15] is used to select the SINR threshold. In this way, the randomness of the decoding process is captured. Figure 3 illustrates this decision process.

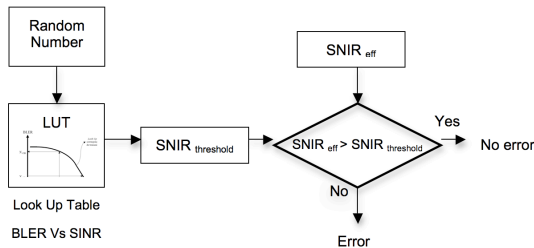


Figure 3: ARQ acceptance process

If the packet is not successfully transmitted after a maximum number of retransmissions ($\max = 3$), the ARQ block is discarded.

3.12 Channel Quality Indicator

The CQI is feed back from the UE to the BS to report the channel state of the OFDMA sub-channels. This information will be used for the BS to select the modulation and coding scheme assigned to the UE in the next OFDMA frame. When the BS is using PUSC, the UE reports the average SINR of all the sub-channels of the BS preamble, while if the BS is using AMC, the UE reports the SINR of the five best sub-channels of the BS preamble [16].

4. TRAFFIC MODELS

In this paper, two different real time services have been used to analyze the performance of DFP under a truly dynamic scenario: VoIP and H.263 Video. In the following, the way in which both traffic services are modeled is shown.

4.1 VoIP

A typical VoIP call can normally be divided into two stages: talking and listening. In the talking period, the user is transmitting packets, while in the listening period, the user is receiving packets. Therefore, a two states Markov chain can be used to model this process.

This kind of approach has been studied in [17], where the parameters and values of such a model can be found. On the one hand, the probability of moving from the active to the inactive state is equal to 0.6, while the probability of changing from the inactive to the active state is 0.4. On the other hand, the period of time that a user is talking is defined by an exponential distribution of mean 1.0 s, while

the period of time that a user is listening is defined by an exponential distribution of mean 1.5 s.

When the user is in the talking state, packets of fix size are generated at regular intervals. The values of these parameters depend on the voice codecs and compression schemes. In this case, a simplified AMR (*Adaptive Multi Rate*) audio data compression technique is used. The payload of the AMR packets is 33 bytes, and they are generated at a rate of 20 ms.

When the user is in the listening state, a comfort noise is generated in order to avoid the confusion of the customer between the listening and disconnected state. The payload of these packets is 7 bytes, and they are generated at a rate of 160 ms.

4.2 H.263 Video

H.263 video is a codec designed for the transmission of low data rates for video-conferencing and video-telephony. This codec uses as a main element a block based *DCT* (*Discrete Cosine Transform*), and three different types of frame: *I-Frame* (*Intra-coded Frame*), which entirely encodes the video image without reference to any other frame; *P-Frame* (*Predictive-coded Frame*), which only encodes the differences between the current and previous video image; *PB-Frame*, which encodes two consecutive frames in one entity.

The I-Frames are transmitted at a constant and deterministic rate. In addition, an I-Frame is always followed by a P-Frame. Therefore, a typical H.263 video session can be modeled by using a two states Markov chain: P-Frame and PB-Frame [18].

In order to evaluate the parameters of the H.263 video model, the H.263 Star Wars video stream has been employed [19]. The probabilities of moving from a P-Frame to a PB-Frame and vice-versa have been derived from this video stream. Moreover, the size and duration of the P-Frame and PB-Frame generated in each state can be derived using this movie. First, the average and variance frame size ($\mu_s \sigma_s$) and duration ($\mu_d \sigma_d$) are obtained from the empirical data. Afterwards, the cumulative density function of the frame size (CDF_s) and frame duration (CDF_d) are calculated.

To obtain the frame size, a random number X_0 is generated from a normal distribution (CDF_N) with the previously estimated frame size average and variance ($\mu_s \sigma_s$). Then, using the random number X_0 and the previously computed CDF_s , the frame size can be estimated (eq. 8).

To obtain the frame duration and maintain the correlation between the frame size and duration, the same random number X_0 and the previously obtained (CDF_d) are used (eq. 9).

$$FrameSize = CDF_S^{-1}(CDF_N(X_0)) \quad (8)$$

$$FrameDuration = CDF_D^{-1}(CDF_N(X_0)) \quad (9)$$

5. EXPERIMENTAL EVALUATION

In this section, the presented WiMAX dynamic system-level simulator is used to analyze the performance of DFP compared to currently used FRSSs.

A non-uniform WiMAX network comprised of five BSs with three sectors each is used in this experimental evaluation. To simulate an uneven distribution of the UE within the scenario, 1 background traffic map and 2 hot spots are used. Note that VoIP and H.263 video users are generated

with in each traffic map according to different average arrival rates: $\lambda_{VoiP}^{BG} = 5$, $\lambda_{VoiP}^{HS1,2} = 10$, $\lambda_{H263}^{BG} = 2.5$ and $\lambda_{H263}^{HS1,2} = 5$. The scenario and the main parameters of the network can be seen in Figure 2 and Table 4.

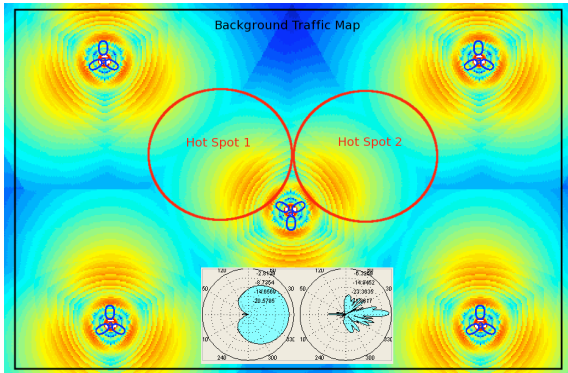


Figure 4: Scenario for Dynamic system-level Simulation

The results of the simulation can be seen in Table 3. These results have been taken from a simulation of 160000 frames of 5 ms each one, which is equivalent to 30 minutes. Note that DFP runs in a frame by frame basis.

When using FRS 1x3x1, since there is no interference coordination, the network suffers from interference, and the number of re-transmission is large due to the low signal quality of the users (Re-tx ratio = 44.22%). However, due to the re-transmissions and the HARQ combining process most of the packets are successfully decoded by the user (Packet loss ratio = 6.85%). Note that the average delay of the network is within acceptable values, from around 1 frame (6.17 ms).

On the other hand, if FRS 1x3x3 is used, interference avoidance is achieved, but the sector capacity is reduced. Because of this, and since the network is highly loaded, most of the packets are delayed and even discarded before transmission due to the lack of resources and the large queuing times. As a result, the average delay of the network (16.30 ms) and the packet loss ratio (19.63%) significantly increases. Note that the number of re-transmissions is small (8.44%), since interference avoidance is provided by the FRS scheme, but also because only a few packets are sent across the network (lot of packets are discarded before transmission).

When using DFP, the different sectors are able to adapt their resources to the users demands and then provide interference avoidance by a sophisticated on-line frequency planning. As a result, the network delay (5.58 ms) and the packet loss (5.22%) are greatly reduced. Note that the re-transmission ratio is not reduced against 1x3x3, the reason behind this is the network traffic. Since DFP reduced the queuing times, many more packets are sent across the network.

Finally, the average network throughput corroborates what has been reveal above. The most sophisticated algorithm, DFP, provides the best network throughput, while the FRSs provide worst results due to the lack of interference coordination or resources.

Note that due to the retransmission, most of the packets are decoded successfully when using 1x3x1. As a result, the throughput carried by the network does not greatly improve

Table 3: SIMULATION RESULTS

Technique	1x3x1	1x3x3	DFP
Packet loss (%)	6.85	19.63	5.22
Re-transmissions (%)	44.22	8.44	20.01
Delay (ms)	6.17	16.30	5.58
Jitter (ms)	3.31	3.86	3.48
Throughput (Mbps)	914.01	620.53	980.51

when using DFP. However, it does decrease the number of retransmissions.

6. CONCLUSION

This paper has introduced a dynamic system-level simulator for WiMAX networks that can be used to analyze the behavior of different interference avoidance techniques. Moreover, the performance of DFP has been compared with off-the-shelf FRSs. DFP has been proven able to provide resource balancing and interference avoidance between sector of the network. DFP reduces the average delay of the network in comparison with such FRSs, which is a key factor for real time services. In addition, it also is able to improve the network throughput, and decrease the number of loss and re-transmission packets.

We are working on the analysis of distributed and dynamic frequency assignment algorithms that will allow DFP to run on a very regular basis on the BS. In this way, the delay of the centralized architecture will be avoided.

7. REFERENCES

- [1] IEEE standard for local and metropolitan area networks: Air interface for fixed broadband wireless access systems- physical and medium access control layers for combined fixed and mobile operation in licensed bands. Technical report, IEEE Std 802.16e-2005, February 2006.
- [2] H. Jia, Z. Zhang, G. Yu, P. Cheng, and S. Li. On the performance of ieee 802.16 ofdma system under different frequency reuse and subcarrier permutation patterns. In *IEEE International Conference on Communications*, volume 24, pages 5720–5725, june 2007.
- [3] S-E. Elayoubi, O. Ben Haddada, and B. Fourestié. Performance evaluation of frequency planning schemes in ofdma-based networks. *IEEE Transactions on Wireless Communications*, 7(5):1623–1633, May 2008.
- [4] D. López-Pérez, A. Jüttner, and J. Zhang. Optimisation methods for dynamic frequency planning in ofdma networks. In *Network 2008*, Budapest, Hungary, September 2008.
- [5] A. Eisenbatter, H.-F. Geerdes, T. Koch, A. Martin, and R. Wessly. Umts radio network evaluation and optimization beyond snapshots. *Mathematical Methods of Operations Research*, 63:1–29, 2005.
- [6] Alvaro Valcarce, Guillaume De La Roche, and Jie Zhang. A GPU approach to FDTD for Radio Coverage Prediction. In *11th IEEE International Conference on Communication Systems*, November 2008.
- [7] F. Aguado Agelet, F. Perez Fontan, and A. Formella. Fast ray tracing for microcellular and indoor

Table 2: SIMULATION PARAMETERS

Parameter	Value	Parameter	Value
Sites	15	CPE Antenna Gain	0 dBi
Sector/site	3	CPE Antenna Pattern	Omni
Carrier Frequency	3.5 GHz	CPE Antenna Height	1.5 m
Channel Bandwidth	10 MHz	CPE Noise Figure	5 dB
DL:UL Ratio	1:1	CPE Cable Loss	0 dB
Permutation Scheme	AMC	Type of Service 1	VoIP
Frame Duration	5 ms	Type of Service 2	H.263video
Sub-channels	48	ARQ block size	128 bytes
DL symbols	19	PDU size	128 bytes
BS TX Power	43 dBm	σ (Shadow Fading)	8 dB
BS Antenna Gain	18 dBi	Intra BS correlation	0.7
BS Antenna Beam Width	90	Inter BS correlation	0.5
BS Antenna Height	30 m	Path Loss Model	Hata
BS Antenna Tilt	3	Fast Fading Model	SUI-4
BS Noise Figure	4 dB	Scheduling	Best SINR
BS Cable Loss	3 dB	HARQ method	CC
CPE Tx Power	23 dBm	OFDMA frames	160000

environments. *IEEE Transactions on Magnetics*, 33(2):1484–1487, March 1997.

- [8] L. Häring, B. K. Chalise, and A. Czylik. Dynamic system level simulations of downlink beamforming for umts fdd. In *Globecom*, 2003.
- [9] L. Reggiani, L. Galati Giordano, and L. Dossi. Multi-user sub-channel, bit and power allocation in iee 802.16 systems. In *VTC2007-Spring*, volume 22-25, pages 3120 – 3124, April 2007.
- [10] Z. Taoo, A. Li, J. Zhang, and T. Kuze. Performance improvement for multichannel harq protocol in next generation wimax systems. In *WCNC*, 2008.
- [11] R. Selea. Arq block size in 802.16. Technical report, IEEE 802.16 Broadband Wireless Access Working Group, April 2004.
- [12] J. G. Andrews, A. Ghosh, and R. Muhamed. *Fundamentals of WiMAX Understanding Broadband Wireless Networking*. Prentice Hall, Massachusetts, 2007.
- [13] Wimax system evaluation methodology. Technical report, Wimax Forum, January 2007.
- [14] Frederiksen, F. Kolding, and T. E. Performance and modelling of wcdma/hsdpa transmission/h-arq schemes. In *VTC*, volume 1, pages 472–476, 2002.
- [15] J. Gozávez. *Performance Analysis of Link Adaptation for Circuit and Packet Switched TDMA Mobile Communications Systems*. PhD thesis, Department of Electronic and Electrical Engineering, University of Strathclyde, 2002.
- [16] T. Kwon, H. Lee, S. Choi, J. Kim, and D.-H. Cho. Design and implementation of a simulator based on a cross-layer protocol between mac and phy layers in a wibro compatible iee 802.16e ofdma system. In *IEEE Communications Magazine*, December 2005.
- [17] W. Lee, J. Choi, K. Ryu, and R. Kim. Draft iee 802.16m evaluation methodology and key criteria for 802.16m – advanced air interface. Technical report, IEEE 802.16 Broadband Wireless Access Working Group, 2007.
- [18] Lazaro O., Girma D., and Dunlop J. H.263 video traffic modelling for low bit rate wireless communications. In *Personal, Indoor and Mobile Radio Communications*, volume 3, pages 2124 – 2128, September 2004.
- [19] Mpeg-4 and h.263 video traces for network performance evaluation.